

# Study on Control-release and Synchronized of Metformin Hydrochloride Drug from Hydrophilic Polymers AgNP/SCC-g-poly (AAc-AAm)

Aseel M. Aljeboree<sup>1</sup>, Nadher D. Radia<sup>2\*</sup>, Zeina M. Kadam<sup>3</sup>, Yahya A. Faleh<sup>4</sup>,  
Usama S. Altimari<sup>5</sup>, Ashour H. Dawood<sup>6</sup>, Ayad F. Alkaim<sup>7</sup>

<sup>1,7</sup>Department of Chemistry, College of Science for Women, University of Babylon, Hilla, Iraq.

<sup>2</sup>Department of Chemistry, College of Education, University of Al-Qadisiyah, Diwaniyah, Iraq.

<sup>3</sup>Department of Chemistry, College of Science, University of Al-Qadisiyah, Diwaniyah, Iraq.

<sup>4</sup>Ministry of Education, Directorate of Education Al-Qadisiyah, Diwaniyah, Iraq.

<sup>5</sup>Department of Pharmacy, Al-Nisour University College, Baghdad, Iraq.

<sup>6</sup>Department of Medical Engineering, Al-Esraa University College, Baghdad, Iraq.

*Received: 19<sup>th</sup> February, 2023; Revised: 15<sup>th</sup> April, 2023; Accepted: 12<sup>th</sup> May, 2023; Available Online: 25<sup>th</sup> June, 2023*

## ABSTRACT

In this study, based on the free radical polymerization, a high-efficiency sodium carboxymethyl cellulose-grafted-Poly (acryl acid-acrylic amide) (SCC-g-Poly (AAc-AAm)) hydrogel was prepared using initiators for the generation of free radicals (KPs) and a cross-linking agent, N,N'-Methylene-bis-acrylamide (MBA) as well as loading silver nanoparticles onto SCC-g-poly (AAc-AAm) hydrogel cross-linked by silver nitrate was added at the concentration (1000 mg/L) for about one day to load silver ions on the surface. utilized this AgNP/SCC-g-poly (AAc-AAm) hydrogel to drug release of metformin hydrochloride (MH) was studied at different acid mediums (pH = 7.4 and 1.2) and temperatures of 37°C. This study then studied the ability of the surface to release silver controlled. Field emission scanning electron microscopy (FESEM), Fourier-transform infrared (FTIR), X-ray diffraction (XRD), transmission electron microscopy (TEM), atomic force microscopy (AFM) as well as Brunauer–Emmett–Teller (BET), were among the techniques used to examine the prepared surface's properties. The highest reported drug release rates occurred at (pH = 7.4) when the rate of drug release was 97.19% after 500 minutes. This is caused by the hydrogel containing COOH, C=O, and OH groups that ionize in the neutral medium (pH = 7.4), forming negative ions, which electrostatically repel each other with the unshared electron pair of the NH group. On the contrary to in an acidic medium (pH = 1.2), the hydrophilic groups included in the hydrogel composition are saturated, making them bond with hydrogen bonds with each other and the percentage of swelling of hydrogel is very small. Two different bacteria species (Gram-negative and Gram-positive bacteria) were used to study the AgNP/SCC-g-poly (AAc-AAm) hydrogel and the ability of the surface to inhibit the two types of bacteria.

**Keywords:** Hydrogel, Metformin hydrochloride drug, Adsorption, Biological activity, Drug release.

International Journal of Drug Delivery Technology (2023); DOI: 10.25258/ijddt.13.2.38

**How to cite this article:** Aljeboree AM, Radia ND, Kadam ZM, Faleh YA, Altimari US, Dawood AH, Alkaim AF. Study on Control-release and Synchronized of Metformin Hydrochloride Drug from Hydrophilic Polymers AgNP/SCC-g-poly (AAc-AAm). International Journal of Drug Delivery Technology. 2023;13(2):708-712.

**Source of support:** Nil.

**Conflict of interest:** None

## INTRODUCTION

Hydrogels are three-dimensional interlocking hydrophilic polymeric networks manufactured from natural or synthetic materials. Hydrogels have a degree of flexibility that is remarkably comparable to live tissue because of their large water content. Therefore, they are suitable to be used in many areas, such as drug delivery, contact lenses, making artificial muscles, tissue engineering, wound dressings, pharmaceuticals, agriculture, as well as the manufacture of hygiene and health care products, such as diapers, water purification, and

decontamination with organic waste.<sup>1-4</sup> Hydrogels swell and contract in response to changes in environmental stimuli, particularly chemical (ionic strength, solvent composition, pH), physical (magnetic or electric field, light, pressure, temperature, sound), as well as biochemical. Apart from that, adsorption is the adhesion or accumulation of atoms, ions, or molecules (liquid or gaseous) on a solid surface and is a physical or chemical bonding of molecules of materials at the active sites of the surface by weak Van der Waals forces, or by forming chemical bonds with the active sites on the surface.<sup>5-9</sup>

\*Author for Correspondence: nadhir.dhaman@qu.edu.iq

It accumulates on the solid surface called the adsorbate, and the surface on which the adsorbent accumulates is called the adsorbent. The cause of the adsorption phenomenon is the presence of unsaturated active site residues on the adsorbent surface. This is due to the binding of an insufficient number of particles on the surface and the appearance of unbalanced intermolecular forces on the solid surface to eliminate these forces as the solid surface tends to attract and retain particles.<sup>10-12</sup> Metformin hydrochloride (MFH) is the most widely prescribed oral drug for the management of type 2 diabetics and used as an anti-diabetic drug. MFH was also utilized as anti-cancer therapy besides uses in the treatment of endocrine disturbances. Recently MFH has been assumed to be among the highest released pharmaceuticals into the aquatic system due to low, high pKa and high mobility in aqueous solutions with the concentration range in domestic wastewater (64–98 g/L).<sup>13,14</sup> Here, we incorporated Ag nanoparticles in the (SCC-g-Poly (AAc-AAm) hydrogel was prepared using initiators for the generation of free radicals .utilized this AgNP/SCC-g-poly (AAc-AAm) hydrogel to drug release of metformin hydrochloride (MH) was studied at different acid mediums (pH = 7.4 and 1.2) and temperatures of 37°C.

## MATERIAL AND METHODS

### Chemicals and Materials

Metformin hydrochloride (MH) is a Samarra company (Iraq) manufactured drug. N, N'-Methylene-bis-acrylamide (MBA), sodium carboxymethyl cellulose (SCC), acrylic amide (AAm), acryl acid (AAc), potassium persulfate (KPS), hydrochloric acid (HCl) and NaOH Sodium hydroxide (0.1N) from Sigma-Aldrich.

### Drug Release

The release of MH hydrogel-loading drug was studied by taking the weight (0.1 gm) of the drug-loading surface in different acidic media (pH = 7.4 and 1.2) at temperature (37 °C) and concentrations (500 mg/L) during different times (15–24 hours).

### Loading of Silver Nanoparticles onto Hydrogel

The mass (0.1 g) of hydrogel in (100 mL) of distilled water and the hydrogel surface are left in distilled water for three days to increase hydrogel swelling. Besides that, silver nitrate was added at the concentration (1000 mg/L) for about one day to load silver ions on the surface. After that, the solution of sodium borohydride (NaBH<sub>4</sub>) was added to reduce silver ions, left in the solution for (24 hours) and then dried to obtain the used powder.

### Biological Activity

The antibacterial effect of nanosilver-loaded hydrogel was tested based on two types of gram-negative and gram-positive bacteria. (Mueller-Hinton agar) was used as a culture medium for bacteria by dissolving (83 g) of agar in (1000 mL) of distilled water at a temperature of (37°C). Note that the disc diffusion method was used to test the effectiveness of the silver-bearing hydrogel on the two types of bacteria.

## RESULT AND DISCUSSION

### FTIR

Figure 1 shows the infrared spectrum of the sodium carboxymethyl cellulose-grafted-Poly (acryl acid-acrylic amide) (SCC-g-Poly (AAc-AAm) hydrogel that appears at the range (3200–3500 cm<sup>-1</sup>). It indicates that there is an interaction between the two hydroxyl groups, OH belonging to sodium carboxymethyl cellulose (SCC), and amine (NH), belonging to acrylamide (AAm). The bands visible within the range (2900–2960 cm<sup>-1</sup>) are of aliphatic CH groups. Other than that, the carbonyl (C=O) group in AAc causes the package to be at (1745 cm<sup>-1</sup>). The C=O group of AAm is responsible for the small peaks in the region (1600–1700 cm<sup>-1</sup>). The COO<sup>-</sup> negative carboxylate ion is stretched symmetrically and asymmetrically, resulting in the peaks at (1396 and 1542 cm<sup>-1</sup>) accordingly. Due to C-N bonding, the peak at (1204 cm<sup>-1</sup>) is present. Note that the C-O-C correlation is seen by the apparent peak at (1010 cm<sup>-1</sup>). The infrared spectrum of AgNP/SCC-g-poly (AAc-AAm) hydrogel can also be observed after loading of silver nanoparticle. It is observed that there is a shift or decrease in the functional group's sites of the hydrogel post-drug adsorption because of an overlap between the functional groups of both the drug and hydrogel.<sup>15</sup>

### X-ray Diffraction

The prepared SCC-g-Poly (AAc-AAm) hydrogel was examined via XRD using an angular range ( $2\theta=10-80$ ) and a wavelength (1.5406 Å). It was observed that a wide band appeared at the angular range ( $2\theta=15-25$ ), especially at the angular range ( $2\theta=20.224^\circ$ ) within the interlayer distance ( $d=4.391\text{Å}$ ), indicating the amorphous nature of the hydrogel as in Figure 2 (a). Meanwhile, in Figure 2 (b) the XRD spectrum of the loaded hydrogel by silver nanoparticles that the intensity decreases at ( $2\theta=20.244^\circ$ ). This indicates the crystalline nature of the hydrogel after silver loading.<sup>16,17</sup>

### FESEM

The results of FESEM are shown in Figure 3(a) hydrogel, (b) hydrogel after the adsorption process, and (c) hydrogel after loading silver nanoparticles. The hydrogel in Figure 3(a) is rough and porous because of the weak bonds before adsorption.

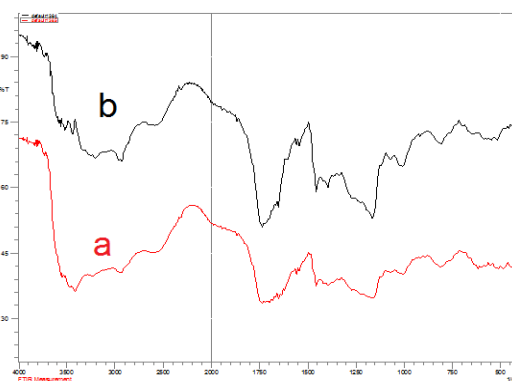


**Figure 1:** FTIR spectra of a) SCC-g-poly (AAc-AAm) hydrogel and b) AgNP/SCC-g-poly (AAc-AAm) hydrogel

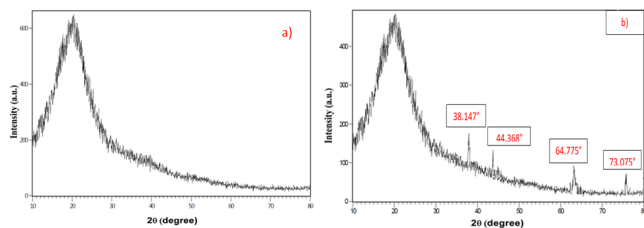


Figure 2: XRD a) SCC-g-P(AAc-AAm) hydrogel and b) AgNP/SCC-g-poly (AAc-AAm) hydrogel

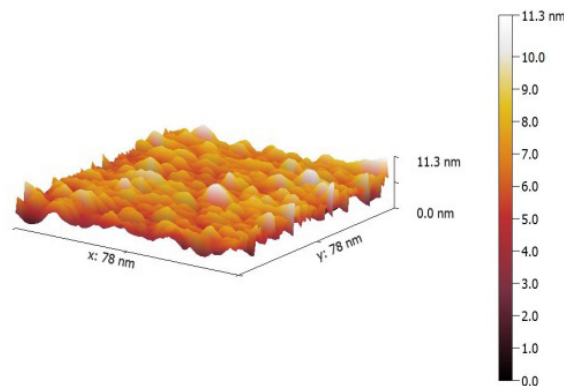


Figure 4: AFM image of SCC-g-P(AAc-AAm) hydrogel

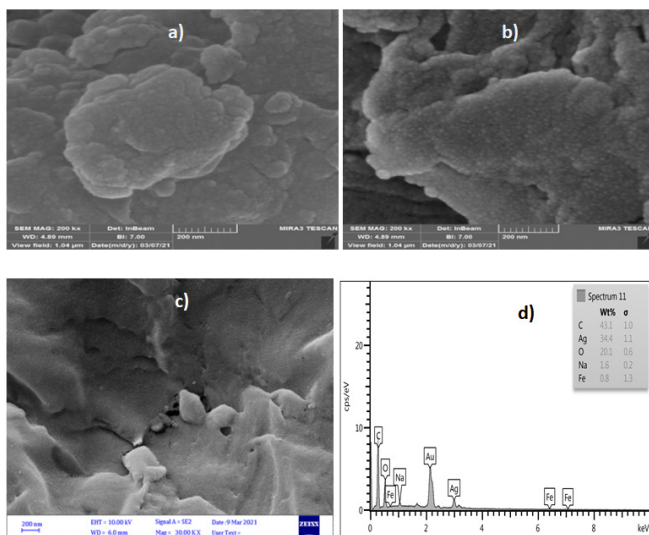


Figure 3: FESEM image a) SCC-g-Poly (AAc-AAm) hydrogel after adsorption, b) after adsorption, c) AgNP/SCC-g-poly (AAc-AAm) hydrogel, and d) EDS of AgNP/SCC-g-poly (AAc-AAm) hydrogel

However, the adsorption process was deemed successful because the hydrogel surface became smooth after the drug particles were filled into the active sites and formed a layer, as illustrated in Figure 3(b).<sup>18</sup> Furthermore, after loading the nanosilver onto hydrogel, the surface became very smooth, as evidenced by nanosilver loading. Therefore, it is to confirm the nanosilver loading on the surface through the energy dispersive X-ray analysis (EDX) technique<sup>19</sup> as in Figure 3 c and d.

### Atomic Force Microscopy

AFM was used through the topography of the SCC-g-Poly (AAc-AAm) hydrogel. It gives three-dimensional images through which we obtain information about the thickness, homogeneity, and surface roughness (surface roughness relative to the square root of mean square roughness (MSR)). The hydrogel surface is porous and rough, evidenced by the high average roughness value. Furthermore, the peaks on the surface are more than the dips, which is evident from the positive value of  $R_{ks}$ . At the positive value of  $R_{ks}$ , the peaks are more than the dips.

On the contrary, at the negative value of  $R_{ks}$ , the peaks are less than the dips. However, if the value of  $R_{ks}$  equals zero, this means there exists a symmetrical distribution of highs and lows at the surface<sup>4</sup> as in Figure 4. Statistical values of hydrogel roughness as show in Table 1.

**Table 1:** Statistical values of hydrogel roughness

<i>CMC-g-P(AAc-AAm)</i>	<i>statistical roughness coefficients (nm)</i>
197.9	$R_a$
237.0	$R_q$
0.9077	$R_{sk}$
3.011	$R_{ku}$
737.0	$R_p$
257.3	$R_v$
994.3	$R_z$

### Transmission Electron Microscopy

TEM images of SCC-g-Poly (AAc-AAm) hydrogel and loading of silver nanoparticle AgNP/SCC-g-poly (AAc-AAm) hydrogel. The hydrogel is semi-transparent, which indicates the homogeneity of the hydrogel components with each other due to the effect of cross-linking agent and bonding with Van der Waals forces. Whereas, once the drug has been loaded onto the hydrogel surface, heterogeneous clumps were observed on the hydrogel surface, representing the gathering of drug molecules adsorbed on the surface.<sup>20</sup> The hydrogel loaded with silver nanoparticles showed that single, non-clumped spherical black dots represent the adsorbed silver particles. Other than that, the nature of the hydrogel chain structure has an important role in stabilizing silver particles and not agglomerating them. This is because there is a coordination between the carboxyl (COOH) and hydroxyl (OH) groups on the one hand and silver particles on the other,<sup>21</sup> as shown in Figure 5.

### Surface Area Analysis and Porosity Nature of Surface (BET, BJH)

The AgNP/SCC-g-poly (AAc-AAm) surface properties have been studied and shown in Figure 6. It shows the BET isotherm for nitrogen gas adsorption for the hydrogel and its pore size distribution. Note that the hydrogel's nitrogen isotherm (adsorption-adsorption) is one of the IV types, the term "IV type" describes the formation of a monolayer, followed by the formation of multiple layers, as well as the characterization of the surface area of mesoporous materials. with multi-layered hysteresis loops of the type (H3). Furthermore, the irregular Barrett-Joyner-Halenda (BJH) pore size and volume analysis

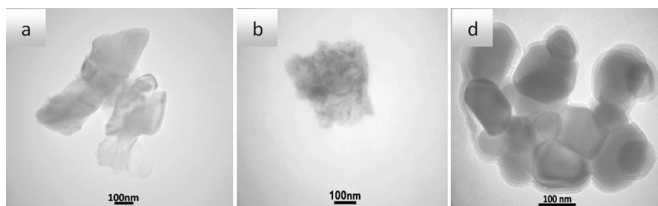


**Figure 5:** (TEM) images of a) SCC-g-P(AAc-Aam) hydrogels, b) after loading drug, and c) AgNP/SCC-g-poly (AAc-AAm) hydrogel

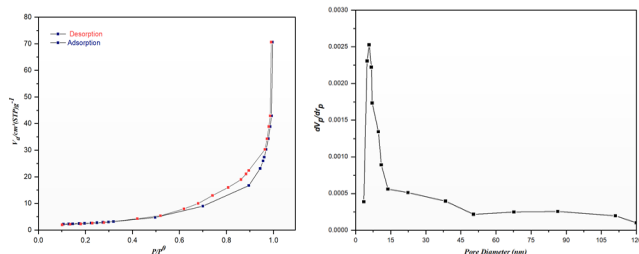


**Figure 6:** Nitrogen adsorption-desorption isotherms and the corresponding pore size distribution curve of AgNP/SCC-g-poly (AAc-AAm)

distribution of the surface pores is shown, i.e., it contains slit-shaped porous pores. BJH for the hydrogel has shown that the surface area is ( $1.7542 \text{ m}^2/\text{g}$ ), the pore volume is ( $0.0029 \text{ cm}^3/\text{g}$ ), and the average pore diameter is ( $7.5610 \text{ nm}$ ).<sup>22</sup>

### Drug Release

The drug release of metformin hydrochloride (MH) from hydrogel was studied at different acid and neutral mediums ( $\text{pH} = 7.4$  and  $1.2$ ) and temperatures of  $37^\circ\text{C}$ , as shown in Figure 7. Note that the best drug release rates were recorded at ( $\text{pH} = 7.4$ ), in which the drug release rate was  $97.19\%$  after 500 minutes. This is caused by the hydrogel containing  $\text{COOH}$ ,  $\text{C=O}$ , and  $\text{OH}$  groups that ionize in the neutral medium ( $\text{pH} = 7.4$ ), forming negative ions, which electrostatically repel each other with the unshared electron pair of the  $\text{NH}$  group. It then causes the hydrogel to swell and thus allows the drug to be released at high rates.<sup>23,24</sup> In an acidic medium ( $\text{pH} = 1.2$ ), tiny swelling percentages of SCC-g-Poly (AAc-AAm) hydrogel were recorded. Other than that, the hydrophilic groups included in the hydrogel composition are saturated, making them bond with hydrogen bonds with each other. Thus, the electrostatic repulsion between these groups decreases, and the hydrogel is in a state of contraction. Subsequently, the percentage of swelling of hydrogel is very small, and the drug release is in a few proportions compared to the release at ( $\text{pH} = 7.4$ ).<sup>25</sup>

### Biological Activity

The antibacterial effect of silver nanoparticles loading onto SCC-g-Poly (AAc-AAm) hydrogel (AgNP/SCC-g-poly (AAc-AAm)) was studied using two types of bacteria, gram-positive (*S. aureus*) and gram-negative (*E. coli*), predicating on the liberating silver process at different times (5, 10, 15 hours). The results are shown in Figure 8, showing the effectiveness of the hydrogel in inhibiting the two types of bacteria. It was discovered that the diameter of the inhibitory zone grows as

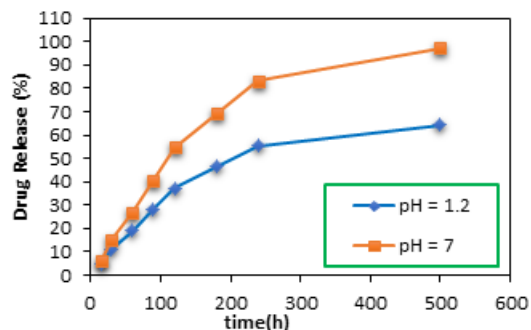


**Figure 7:** Drug Release profiles of Metformin hydrochloride from the SCC-g-Poly (AAc-AAm) hydrogel in  $\text{pH} 1.2$  and  $\text{pH} 7.4$  at  $37 \pm 0.5^\circ\text{C}$

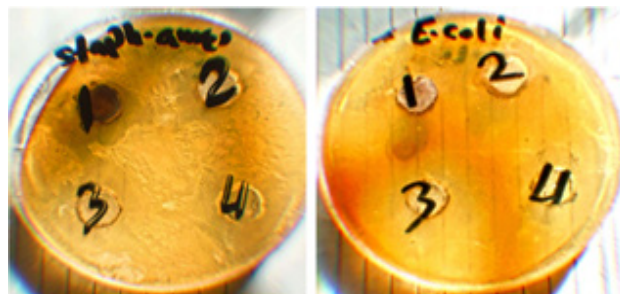


**Figure 8:** Antibacterial activity of two bacteria using disc diffusion method at a different time of liberating silver.

the silver liberation time rises. This condition is greater for gram-negative bacteria (for example, *E. coli*) than for gram-positive bacteria (*S. aureus*).<sup>26-29</sup>

### CONCLUSION

Loading silver nanoparticles on the hydrogel surface were cross-linked, and the ability of the surface to release silver controlled was also studied. The prepared hydrogel has a high swelling rate at ( $\text{pH} = 7.4$ ), and the highest rates of metformin hydrochloride (MH) drug release loaded on the hydrogel were recorded at a  $\text{pH} = 7.4$ . The prepared hydrogel loaded with silver nanoparticles AgNP/SCC-g-poly (AAc-AAm) hydrogel showed clear biological activity to inhibit gram-positive and Gram-negative bacteria.

### REFERENCES

1. Attia AA, Girgis BS, Fathy NA. Removal of methylene blue by carbons derived from peach stones by  $\text{H}_3\text{PO}_4$  activation: Batch and column studies. *Dyes and Pigments*. 2008; 76(1):282-289.
2. Alkaim AF, Ajobree AM. White marble as an alternative surface for removal of toxic dyes (Methylene blue) from Aqueous solutions. *International Journal of Advanced Science and Technology*. 2020; 29(5):5470-5479.
3. Alwan NA, Kadam ZM. Preparing and diagnosing the biological activity of some metallic complexes with ligand 4-Benzophenol Azopyrogallol(4). in *IOP Conference Series: Earth and Environmental Science*. 2021; 28:1-8.
4. Adriano WS, Veredas V, Santana C C, Goncalves LR. Adsorption of amoxicillin on chitosan beads: Kinetics, equilibrium and validation of finite bath models. *Biochemical Engineering Journal*. 2005; 27(2): 132-137.
5. Ahmed M, Abdelghany A, Nabil M A, Patrice R M. Efficiently

- activated carbons from corn cob for methylene blue adsorption. *Applied Surface Science Advances*. 2021;2: 100037.
6. Ruihua M , Xi CN , Ning W , Jing Y . *Hydrogel adsorbent in industrial wastewater treatment and ecological environment protection*. *Environmental Technology & Innovation*. 2020; 20: 101-107.
  7. Aljeboree AM, Alshirifi AN ,Alkaim AF . *Removal of pharmaceutical amoxicillin drug by using (Cnt) decorated clay/ fe2 o3 micro/nanocomposite as effective adsorbent: Process optimization for ultrasound-assisted adsorption*. *International Journal of Pharmaceutical Research*.2019; 11(4):80-86.
  8. Wared SHH, Radia ND. Synthesis and characterization of sodium alginate-g-polyacrylic acid hydrogel and its application for crystal violet dye adsorption *International Journal of Drug Delivery Technology*. 2021; 11(2):56-565.
  9. Zaied AM, Ali TB, Aseel MA, Ayad FA. *Adsorption and removal of textile dye (methylene blue mb) from aqueous solution by activated carbon as a model (apricot stone source waste) of plant role in environmental enhancement*. *Plant Archives*. 2019;19: 910-914.
  10. Aljeboree AM, Alkaim AF, Loay A, Algburi HM. *Photocatalytic degradation of textile dye cristal violet wastewater using zinc oxide as a model of pharmaceutical threat reductions*. *Journal of Global Pharma Technology*. 2019;11(2):138-143.
  11. Abdtawfeeq TH, Farhan ZA, Al-Majdi K, Jawad MA, Zabibah RS, Riadi Y, Hadrawi SK, AL-Alwany A, Shams MA, Ultrasound-Assisted and One-Pot Synthesis of New Fe3O4 / Mo-MOF Magnetic Nano Polymer as a Strong Antimicrobial Agent and Efficient Nanocatalyst in the Multicomponent Synthesis of Novel Pyrano[2,3-d]pyrimidines Derivatives, 2023, 33 (2): 472–483, DOI: 10.1007/s10904-022-02514-7
  12. Aljeboree AM, Alkaim AF. Comparative removal of three textile dyes from aqueous solutions by adsorption : As a model (corn-cob source waste) of plants role in environmental enhancement. *Plant Archives*.2019; 19(1):1613-1620.
  13. Nadher DR, Suhair MHK, Hadeer J , Russul R A, Samar E I , Mohammed S A , Sukaina T G , Aseel M A . *Role of Hydrogel and Study of its High-Efficiency to Removal Streptomycin drug from Aqueous Solutions*. *International Journal of Pharmaceutical Quality Assurance*. 2022; 13(2): 160-163.
  14. Ruihua M , Xi CN , Ning W , Jing Y . *Hydrogel adsorbent in industrial wastewater treatment and ecological environment protection*. *Environmental Technology & Innovation*. 2020; 20: 101-107.
  15. Yao Y, Bing H, Feifei X, Xiaofeng C. *Equilibrium and kinetic studies of methyl orange adsorption on multiwalled carbon nanotubes*. *Chem. Eng. J*. 2011; 170(1):82-89.
  16. Al-Mashhadani Z I. Antibiotics Removal by Adsorption onto Eco-friendly Surface: Characterization and Kinetic Study. *International Journal of Pharmaceutical Quality Assurance*. 2021; 12(4):252-255.
  17. Yazidi A A, Felycia S L, Smadji E S, Alessandro B P, Guilherme Ben .*Adsorption of amoxicillin and tetracycline on activated carbon prepared from durian shell in single and binary systems: Experimental study and modeling analysis*. *Chemical Engineering Journal*. 2020; 379: 122320.
  18. Yao Y, Bing H, Feifei X, Xiaofeng C. *Equilibrium and kinetic studies of methyl orange adsorption on multiwalled carbon nanotubes*. *Chem. Eng. J*. 2011; 170(1):82-89.
  19. Nadher D R, Ahmed B M , Ghufraan A M, Abeer S , Usama S A, Marwah A S, Aseel M A , Firas H A .*Removal of Rose Bengal Dye from Aqueous Solution using Low Cost (SA-g-PAAc) Hydrogel: Equilibrium and Kinetic Study*. *International Journal of Drug Delivery Technology*. 2022; 12(3):957-960.
  20. Ahmed M, Abdelghany A ,Nabil M A ,Patrice R M. *Efficiently activated carbons from corn cob for methylene blue adsorption*. *Applied Surface Science Advances*. 2021;2: 100037.
  21. Ruihua M , Xi CN , Ning W , Jing Y . *Hydrogel adsorbent in industrial wastewater treatment and ecological environment protection*. *Environmental Technology & Innovation*. 2020; 20: 101-107.
  22. Aljeboree AM, Alshirifi AN, Alkaim AF. Activated carbon (as a waste plant sources)-clay micro/nanocomposite as effective adsorbent: Process optimization for ultrasound-assisted adsorption removal of amoxicillin drug. *Plant Archives*.2019;19: 915 – 919.
  23. Al-Mashhadani Z I. Antibiotics Removal by Adsorption onto Eco-friendly Surface: Characterization and Kinetic Study. *International Journal of Pharmaceutical Quality Assurance*. 2021; 12(4):252-255.
  24. Lian Z. Plasmonic silver quantum dots coupled with hierarchical TiO2 nanotube arrays photoelectrodes for efficient visible-light photoelectrocatalytic hydrogen evolution. *Scientific reports*. 2015; 5(1):1-10.
  25. Abdulsada G J, Kadam ZM. Improvement the Chemical Structure, Optical and Magnetic Properties of CuFe2O4 Thin Films. *ARPN Journal of Engineering and Applied Sciences*.2019;14(8): 10251-10255.
  26. Aljeboree A M, Essa S M,Kadam Z M.,Dawood F A.,Falah D ,Alkaim A F. *Environmentally Friendly Activated Carbon Derived from Palm Leaf for the Removal of Toxic Reactive Green Dye*. *International Journal of Pharmaceutical Quality Assurance*.2023; 14(1):. 12-15.
  27. Patra J K , Baek KH . *Antibacterial activity and synergistic antibacterial potential of biosynthesized silver nanoparticles against foodborne pathogenic bacteria along with its anticandidal and antioxidant effects*. *Frontiers in microbiology*.2017; 8(2):22-29.
  28. Hoidy WH. *Synthesis, characterization and evaluation of biological activity of corn oil-based difatty acyl carbamodithioic acid*. *Research Journal of Pharmacy and Technology*. 2023;13(4):1931-1935.
  29. AguzzC , Capra p,Bonferoni C ,Cerezo P,Salcedo I ,Snchez R, Caramella C ,Viseras C. *Chitosan silicate bio composites to be used in modified drug release of 5-aminosalicylic acid (5-ASA)*. *Applied Clay Science*. 2020; 50(1): 106-111.